PCCP

Accepted Manuscript

ROYAL SOCIETY OF CHEMISTRY

www.rsc.org/pccp

Supported Lipid Bilayer Repair Mediated by AH Peptide

Min Chul Kim[†,‡], Anders Gunnarsson[‖], Seyed R. Tabaei[†,‡], Fredrik Höök[‖], and Nam-Joon Cho*[†,‡,§]

[†]School of Materials Science and Engineering, Nanyang Technological University, 50 Nanyang Avenue 639798, Singapore
[‡]Centre for Biomimetic Sensor Science, Nanyang Technological University, 50 Nanyang Drive 637553, Singapore
[§]School of Chemical and Biomedical Engineering, Nanyang Technological University, 62 Nanyang Drive 637459, Singapore
[‖]Department of Applied Physics, Chalmers University of Technology, Gothenburg, Sweden

*To whom correspondence should be addressed:

Nanyang Associate Professor Nam-Joon Cho
School of Materials Science and Engineering
Nanyang Technological University
50 Nanyang Avenue 639798, Singapore
E-mail: njcho@ntu.edu.sg

Keywords: lipid vesicle, supported lipid bilayer, quartz crystal microbalance-dissipation, fluorescence microscopy, AH peptide, surface functionalization

Abstract

The adsorption and fusion of small unilamellar lipid vesicles on silica-based substrates such as glass is a common method to fabricate supported lipid bilayers. Successful bilayer formation depends on a number of experimental conditions as well as on the quality of the vesicle preparation. Inevitably, a small fraction of unruptured vesicles always remains in a supported bilayer, and this kind of defect can have devastating influences on the morphological and electrical properties of the supported bilayer when used as a biosensing platform. Here, we report a simple method to improve the completeness of supported bilayers by adding a vesicle-rupturing peptide as a final step in the fabrication process. Peptide treatment reduces the fraction of unruptured vesicles to less than 1%, as determined by epifluorescence microscopy and quartz crystal microbalance-dissipation (QCM-D) experiments. This protocol step can be easily incorporated into existing procedures for preparing high-quality supported lipid bilayers.

Introduction

Formation of planar lipid bilayers on solid supports using phospholipid self-assembly is broadly utilized in scientific research as a versatile means to generate biomimetic model platforms enabling detailed studies of highly complex biological cell membranes[1, 2]. Progress made since the first discovery of the successful formation of a model membrane mimicking cell membranes[1] has opened up a large variety of applications ranging from understanding fundamental phenomena of cellular membranes to highly advanced biomedical assays, including cell culture platforms[3, 4, 5, 6], biosensor development[3, 4], drug screening[4, 5] and medical diagnostics[6].

A large number of model membrane platforms has been explored, including the polymer-cushioned lipid bilayer[5, 7], tethered lipid bilayer[8, 9], black lipid bilayer[10, 11]and planar lipid bilayer[12-15]. Among the options, the planar supported lipid bilayer (SLB) has gained high popularity due to its high stability and the relatively simple procedures by which it can be formed[12, 15]. SLBs are typically produced by either Langmuir-Blodgett (LB) deposition[16] , solvent-assisted lipid bilayer (SALB) formation method[17-22] or surface-mediated vesicle fusion[23]. While LB deposition requires advanced equipment and several steps to sequentially transfer lipid monolayers to the solid substrate, the vesicle fusion method simply utilizes vesicle adsorption, followed by spontaneous rupture when a critical vesicle coverage has been reached on certain hydrophilic substrates including mica, glass or other silica-based surfaces[24]. For the vesicle fusion method, the pathways to cause vesicle rupture-forming lipid bilayers on solid supports are complex, and representative parameters responsible for vesicle fusion and rupture are numerous and include vesicle size[22], lipid composition[25], osmotic pressure[26], ionic strength[27], temperature[28], solution pH[29] and the presence of divalent cations[30].

Based on the aforementioned parameters, the interactions between lipid vesicles and solid supports can be tuned in order to promote or inhibit vesicle rupture leading to SLB formation. Nevertheless, the quality of the SLB with respect to defect density, lateral mobility and the remaining number of non-ruptured vesicles may vary not only from situation to situation but also when attempts are made to perfectly reproduce identical experimental conditions. The imperfections may create significant fractions of inhomogeneity within the bilayer, which may in turn produce short circuits interrupting the measurement of electrical properties of membrane-bound channels[31] and also create artifacts when conducting fluorescence-based bilayer related assays.

Herein, we present a simple method to improve the completeness of supported lipid bilayers through a repair step that is aided by the capacity of an amphipathic α-helical (AH) peptide to induce vesicle rupture[32-34]. In a series of publications[20, 33, 34, 35, 36, 37, 38] from our groups and others, the capacity of this AH peptide to promote SLB formation has been explored, in particular on substrates[32, 33, 35, 36] and lipid compositions[15, 34, 37, 38] that are not compatible with vesicle adsorption-induced SLB formation[15, 34, 37, 38]. For example, Hardy *et al.* succeeded in employing the AH peptide to rupture HIV lipid envelope-mimicking vesicles into SLBs containing high fractions of cholesterol[39], recently extended by exploring concentration-dependent behaviors of SLB-peptide interactions using atomic force microscopy[40]. It has also been shown that using a tethered unilamellar vesicle assay with single-vesicle resolution, 100 nM AH peptide caused single zwitterionic lipid vesicles to rupture at rates that were inversely related to the vesicle diameter[41-43] and similar vesicle-rupture behavior was also observed with another related peptide analogue[38]. Inspired by these reports, we have in this work explored the possibility of using the AH peptide to repair inevitably occurring imperfections in SLBs generated using the vesicle fusion method. The AH peptide-controlled SLB repair process was investigated using the quartz crystal

microbalance with dissipation (QCM-D) monitoring and epifluorescence microscopy techniques. Particular emphasis was put on exploring the possibility to generate high-quality and complete supported lipid bilayers utilizing lipid vesicles with increasing geometrical dimensions. Collectively, this new repair method is anticipated to provide an attractive tool towards creating a defect-free supported lipid bilayer as a broad platform for various bioanalytical applications.

Materials & Methods

Vesicle Preparation. Various populations of lipid vesicles composed of 1-palmitoyl-2-oleoyl-*sn*-glycero-3-phosphocholine (POPC) lipid (Avanti Polar Lipids, Alabaster, AL) were prepared by the extrusion method[44]. Vesicles were extruded by using a Mini Extruder (Avanti Polar Lipids) through track-etched polycarbonate membranes (Whatman Schleicher & Schuell, Dassel, Germany) with pores ranging from 50 to 400 nm diameter. POPC lipids dissolved in chloroform were dried under a gentle stream of nitrogen gas and kept in vacuum to remove any remaining chloroform residue. To create various sizes of unilamellar vesicles, the vesicles were passed through the different-size pore membranes between 7 to 27 times by using the Mini Extruder. Each vesicle suspension was diluted to 0.2 $mg \cdot mL^{-1}$ before experiment. An aqueous buffer solution of 150 mM NaCl and 10 mM Tris in 18.2 MΩ·cm Milli-Q-treated water (Millipore, MA, USA) at pH 7.5 was used in all measurements.

Peptides Reagent. The amphipathic, α-helical (AH) peptide was synthesized by Anaspec Corporation (San Jose, CA). The sequence of AH peptide is H-Ser-Gly-Ser-Trp-Leu-Arg-Asp-Val-Trp-Asp-Trp-Ile-Cys-Thr-Val-Leu-Thr-Asp-Phe-Lys-Thr-Trp-Leu-Gln-Ser-Lys-Leu-Asp-Tyr-Lys-Asp-NH_2. The peptide was prepared and diluted in Tris buffer before the measurements.

Dynamic Light Scattering. Dynamic light scattering (DLS) measurements were conducted on a 90Plus Particle Size Analyzer with a 658.0 nm monochromatic laser (Brookhaven

Instruments Corporation, NY, USA) to measure size distributions of extruded vesicles. Every measurement was taken at a scattering angle of 90° at 25 °C. The light scattering data were collected by digital autocorrelator software (Brookhaven Instruments Corporation). In order to check for multi-modal distributions and to calculate the intensity-weighted Gaussian profile of various size distributions including average effective diameter and polydispersity, all autocorrelation functions acquired were analyzed by CONTIN and Non-Negatively Constrained Least Squares (NNLS) algorithms. Size distributions of each vesicle size are presented in Figure S2.

Quartz Crystal Microbalance-Dissipation (QCM-D) Measurements. Adsorption kinetics and properties of the adsorbed layer were monitored using the quartz crystal microbalance-dissipation (QCM-D) technique with a Q-Sense E4 instrument (Q-Sense AB, Gothenburg, Sweden). In QCM-D experiments, the resonance frequency and energy dissipation of the quartz crystal can be simultaneously obtained[15]. Silicon oxide-coated QCM crystal sensor chips (AT-cut quartz crystals) (Q-Sense) were used for each measurement. Before experiment, the crystals were treated with oxygen plasma using a Plasma Cleaner (Harrick Plasma, Ithaca, NY) at 80 W for 5 min. Experimental data were measured at various overtones (n = 3, 5, 7, 9 and 11), and corresponding changes in resonance frequency and energy dissipation were monitored. The obtained experimental data from the third to seventh overtones were fitted to the Sauerbrey model in order to calculate the effective thickness of the adsorbed layer[36].

Epifluorescence Microscopy. Epifluorescence imaging of supported lipid bilayers formed on a glass substrate was done with an inverted optical microscope (Eclipse TI-U microscope; Nikon, Japan). Imaging was done by using a 60x magnification (NA=1.49) oil immersion objective (Nikon) for measurements resulting in a camera pixel size of 0.267 x 0.267μm. iXon 512x512 pixel EMCCD camera (Andor Technology, Northern Ireland) was used to

capture the fluorescence images, and a fiber-coupled mercury lamp (Intensilight C-HGFIE; Nikon) was used to excite the fluorophores. A TRITC filter was used to filter out the excitation light and the emission light from the measurements with Rh-PE fluorophores.

Fluorescence Recovery after Photobleaching (FRAP). To conduct fluorescence recovery after photobleaching (FRAP) measurements, a circular spot of 20 μm diameter was photobleached for 5 sec by a 532 nm, 100mW laser (Klastech, Germany). Fluorescence micrographs were imaged for 90 sec at one sec interval, and the corresponding lateral diffusion coefficients were obtained based on the Hankel transform method[45].

Results and Discussion

The mechanism of vesicle fusion includes a complex sequence of steps involving vesicle adsorption, deformation, fusion, and rupture leading to reassembly that may eventually result in SLB formation (Figure 1A and Figure S1). Figure 1B presents a typical fluorescence micrograph of a good-quality SLB (Figure S1C). However, even under optimal fabrication conditions, it is our experience that there always remain a number of unruptured or entrapped vesicles in the SLB, which can be easily visualized using epi- or total internal reflection-fluorescence microscopy measurements[46], as illustrated in Figures 1C-E. Upon SLB formation on silica using vesicles with a mean diameter of ca. 91 nm composed of POPC lipid, a significant number (1,000 per 136×136 μm^2) of unruptured vesicles remained bound also after extensive rinsing, either in Tris buffer or in deionized water, the latter of which induces a large osmotic pressure difference that could tentatively aid vesicle removal and SLB repair[26] (Figure 1C, D). The limited effect obtained by rinsing in deionized water highlights that incomplete rupture or imperfect formation of SLB is common not only when there are large unruptured vesicles[47], but also when SLBs are formed using small vesicles (diameter less than 100 nm, See Figure S2 for vesicle size distribution) owing to steric effect in saturated adlayers. Hence, a post-assembly repair method that could aid the formation of

defect-free SLBs would be highly desirable.

Repair of unruptured trapped vesicles within SLBs

Based on the aforementioned studies[15, 33-35, 37, 38, 41], it may be possible to rupture the bound vesicles trapped on the initially formed lipid bilayer by AH peptide. We have previously proposed a mechanism for AH peptide-mediated transformation of intact vesicles into a supported lipid bilayer by simultaneous QCM-D and optical reflectometry measurements[33]. Using the combined techniques, we could monitor the time-dependent variation in adsorbed molecular mass (optical mass), adsorbed molecular mass and solvent mass (acoustic mass), effective thickness, and effective reflective index of the lipid adlayer during the course of the AH peptide interaction with surface-adsorbed lipid vesicles. Briefly, the process of AH peptide-induced vesicle to bilayer transformation comprises three steps: 1) AH peptide binding to vesicles, 2) swelling of vesicles 3) desorption of AH peptide and lipids resulting in formation of an adlayer with a thickness of ~5.1 nm and an effective refractive index of~1.45, which are in very good agreement with expected values for a lipid bilayer. In order to explore this possibility, we utilized the QCM-D technique for tracking the kinetic changes upon addition of AH peptide and subsequent interaction with trapped unruptured vesicles. To obtain a sufficient number of unruptured vesicles trapped on and within the bilayer, we intentionally fabricated large vesicles (~220 nm) for substrate deposition as shown in Figure 2A and B. Upon injection of large-size vesicles onto the silicon oxide substrate, we typically observed two-step kinetics[25] indicative of reaching a critical surface coverage of adsorbed vesicles before the fusion and rupture processes were initiated. However, during the latter process, vesicles were continuously adsorbed onto the substrate which is evidenced by the frequency decrease and dissipation increase after the first peak. Upon subsequent injections of Tris buffer, the frequency shift increased from -65.3 Hz to -37 Hz and the energy dissipation shift decreased from 12.2 to 4.0×10^{-6} (Figure 2A-B), demonstrating suppressed

vesicle adsorption and that a significant fraction of adsorbed unruptured vesicles were rinsed off. Nevertheless, the final changes in Δf and ΔD still deviated significantly from those corresponding to a complete SLB under (Δf ~ 26 Hz and ΔD ~ 0 x 10^{-6})[15], which indicates that a significant fraction of unruptured vesicles remained entrapped on the bilayer. To independently verify this suspicion, we employed epifluorescence microscopy to visualize unruptured vesicles, which were clearly visible as bright dots surrounded by a uniform lipid bilayer (Figure 1C-E). Taking the contribution to the frequency shift originating from coupled water into account,[48] the vesicle coverage estimated by the two methods are in good agreement with each other.

In order to promote complete SLB formation or repair the defects, 8 μM AH peptide were added to the bilayer, and time-sequential fluorescence micrographs were captured as shown in Figure 2D. In addition, as a result of the peptide injection (see arrow 3 in Figure 2A-B), the saturated QCM-D response upon peptide injection corresponded to the responses expected for a complete SLB,[24] i.e. Δf ~ -26 Hz and ΔD ~0×10^{-6} (Figure 2A-B). In order to further characterize the properties of the resulting adlayer, we applied the Sauerbrey model[36] to compute the effective thickness of the adlayer. For the calculations, 1,000 kg·m^{-3} was assumed as the density of the adlayer [36]. The Sauerbrey thickness for the different overtones reached saturation at ~12.7, ~10.9, and ~6.2 nm, respectively (Figure 2C). As a result of AH peptide-mediated repair, the end-resulting thickness of the SLB obtained from the Sauerbrey was resulted at ~4.2 nm indicating that a complete SLB is formed with the aid of AH peptide. Further to confirm the successful repair, the process of AH peptide-mediated rupturing of the remaining vesicles was visualized using a small fraction (0.5 mol %) of Rhodamine-labeled lipid vesicles imaged using epifluorescence microscopy, as shown in time-sequential micrographs (Figure 2C). The AH peptide was injected after the vesicle fusion of large size vesicles (ca. ~188 nm diameter) and a subsequent buffer washing step. The presented

micrographs show time-lapsed images after AH-peptide injection. After peptide injection, a vast majority of trapped vesicles were ruptured, signaling efficient repair of the SLB. The epifluorescence images were captured for a total of ~ 50 min after the injection and each frame of the sequential micrographs is shown at an interval of ~ 5.6 min. Note that there is a large deviation in time scales between that of QCM-D kinetic profiles and epifluorescence imaging, which is attributed to the different measurement chamber geometries and corresponding flow conditions and possibly also the different substrates (glass versus sputtered SiO_2).

To confirm the retainment of lateral diffusivity after AH-peptide addition, FRAP measurements were conducted before and after the repair as shown in Figure 3. It was confirmed that lipid mobility was still retained with a moderate drop of the diffusion coefficient from ~2.3 $\mu m^2 \cdot s^{-1}$ to ~0.9 $\mu m^2 \cdot s^{-1}$, but still displaying a mobile fraction of 89 % as shown in Figure 3B. The decrease in lateral diffusivity of the SLB is likely due to a small fraction of bound AH peptide[35].

As a final verification of the repair process, we investigated if an AH peptide-treated zwitterionic SLB remained resistant to nonspecific adsorption of bovine serum albumin (BSA).[49] Since BSA protein binding was not detectable using the QCM-D technique, the orders of magnitude higher sensitivity offered by epifluorescence microscopy was used to probe the binding of fluorescently labeled BSA upon addition the SLB either without or with prior AH peptide treatment and the amount bound was quantified by the fluorescence intensity per unit area (Figure S3A). In both cases, protein adsorption was minimal and is consistent with AH peptide-mediated vesicle rupture leading to localized SLB formation, which in turn improves the completeness of the SLB platform as a whole. As a control, BSA adsorption onto the bare glass substrate was also tested and, as expected, there was a significantly larger amount of adsorbed protein. There was a greater than 30-fold reduction in

adsorbed proteins to the SLBs versus the glass substrate, verifying that AH peptide treatment preserves the anti-biofouling properties of zwitterionic SLBs (Figure S3B). The collective set of measurement data indicates that AH peptide-mediated SLB repair acts via converting adsorbed, unruptured vesicles into SLB fragments that fill in the defect sites (i.e., the sites of previously unruptured vesicles), leading to a complete and homogenous SLB platform.

Vesicle size-dependent SLB formation and repair

The repair ability of AH peptide was further tested for supported lipid bilayers formed using a broad range of lipid vesicles sizes ranging from ~90 to ~800 nm. Smaller vesicles with a diameter less than 100 nm were previously demonstrated to rupture and form an essentially complete bilayer whereas larger vesicles tend to form mixed layers of SLB fragments with a high number of entrapped vesicles[24]. Here, we focus our attention on addition of AH peptide after vesicle adsorption and monitored the corresponding changes in the kinetics of vesicle rupture upon the addition of AH peptide for different vesicle sizes. In order to explore in detail the effects of differently sized vesicles on AH peptide mediated repair, adsorption kinetic profiles from QCM-D measurements were set to zero after the initial vesicle adsorption and fusion step and subsequent rinsing in buffer (Figure 4). It was shown that the kinetics of AH peptide mediated repairing occurs in a vesicle size-dependent manner, displaying a trend in terms of Δf and ΔD increasing from ~2.4 to ~20 Hz and ~0.3×10^{-6} to ~11×10^{-6}, respectively, for vesicles increasing in size from ca. 91.1 nm to 785.6 nm (Figure 4 and Table 1). The trend of increasing frequency and dissipation shifts with larger vesicle sizes is attributed to both the number of unruptured vesicles which tends to increase with vesicle size as well as the size of individual vesicles which leads to a greater response per vesicle upon AH peptide-mediated rupture. Indeed, the measurement signatures are interpreted as a direct consequence of efficient AH peptide-induced rupture of vesicles trapped in the initially formed SLB. Thus, it was demonstrated that the AH peptide can act as

a broadly applicable repair agent of trapped vesicles even in unfavorable conditions for SLB formation.

SLB repair pathway

To gain further insight into the repair process, the vesicle size-dependent repair mediated by AH peptide was imaged (Figure 5A-C and Movies S1-S3), and the corresponding numbers of unruptured vesicles before and after repair were estimated based on a fluorescence threshold (Figure 5D). Three different SLBs formed using various sizes of vesicles showed distinctive characteristics. For the case of ~ 90 nm (Figure 5A), a much lower number of unruptured vesicles was observed compared to the other bilayers formed using larger sizes of vesicles. This is consistent with previously reported findings that smaller vesicles easily rupture to form a relatively complete bilayer, while larger vesicles tend to form a mixed layer of SLB and intact vesicles[47]. Regardless of the size of vesicles used to form the bilayer, all three cases investigated (91.1, 141.6 and 187.79 nm) resulted in less than ~10 unruptured or trapped vesicles per field of view (136×136 μm^2) on the bilayer after treatment with AH peptide. From the fluorescence micrographs, features signaling a structural transformation of the intact vesicles upon binding with AH peptide was observed (see Movie S1-S3). This experimental finding supports the previously reported mechanism[32] that vesicle rupture mediated by AH peptide is caused by expansion/swelling of intact vesicles, which was here observed to include creation of microvilli or finger-like structures on the outer leaflet of the vesicles. The kinetic profiles from QCM-D measurements (cf. Figure 2A and 4A) are consistent with a structural transformation, although structural details cannot be revealed from ensemble averaging data alone.

Conclusion

Collectively, the experimental findings and analytical results presented here demonstrate a post-assembly repair process mediated by AH peptide allowing the generation of a complete

and homogenous supported lipid bilayer with somewhat reduced but still retained lateral fluidity. This is the first report in which AH peptide is reported to repair defects on supported lipid bilayers formed via vesicle fusion, demonstrating complete SLBs with a negligible amount of unruptured vesicles. This method can be applied to form supported lipid bilayers using large size vesicles which typically cause steric hindrance that disrupts complete rupture of absorbed vesicles. Although further electrical measurements are needed in order to evaluate the insulating properties of AH peptide-treated bilayers,, this new SLB repair approach can improve the feasibility of supported lipid bilayers as a biosensor platform, particularly in cases where high-quality SLBs are needed. It might also be an interesting means to form planar supported lipid bilayers from native cell membranes, which attracts increased attendance in membrane-protein chromatography applications.

Acknowledgments

The authors wish to acknowledge support from the National Research Foundation (NRF-NRFF2011-01 and NRF2015NRF-POC0001-19) and the Swedish Research Council.

Figures

Figure 1. Formation of supported lipid bilayer on glass substrate and its experimental defective cases. Schematics of **(A)** an overall process of supported lipid bilayer formation via vesicle fusion method on the glass substrate and its possible results after the critical vesicle rupture and following buffer washing. Supported lipid bilayer was formed on a glass substrate via vesicle fusion method using 30 nm sized membrane filtered lipid vesicles. Herein, good and defective cases of planar lipid bilayer fluorescence images are presented, **(B)** complete lipid bilayer and **(C-E)** unruptured vesicles trapped on bilayers. After the rupture of the adsorbed vesicles, the lipid bilayer was washed with three different solvents, **(C)** initial Tris buffer (10 mM Tris, 150 mM NaCl and pH 7.5) **(D)** Milli-Q water and **(E)** Tris buffer (10mM Tris, 1 M NaCl and pH 7.5). Note that fluorescence image traces of each washing process were collected for 15 minutes. Each scale bar represents 20 μm.

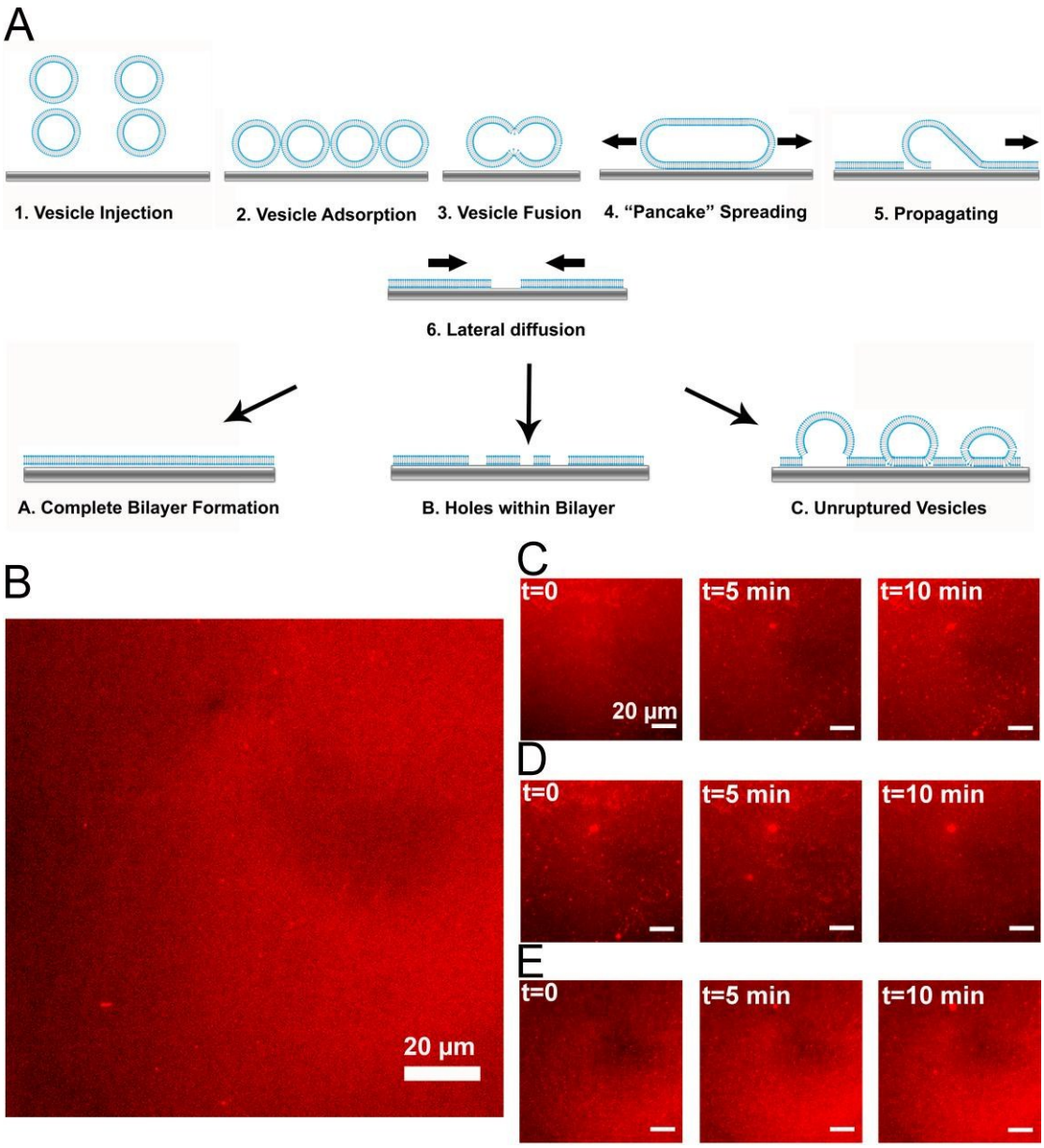

Figure 2. SLB formation and its repairing mediated by AH peptide. After the vesicle (diameter ~ 222.1 nm) adsorption, initial rupture and AH peptide injection, changes in **(A)** resonant frequency and **(B)** energy dissipation were monitored. **(C)** Sauerbrey thickness of the adlayer. n = 3 (black line), n = 5 (red line), and n = 7 (blue line) overtones. **(D)** Time-lapse fluorescence micrographs of AH peptide-mediated SLB repair formed by 188-nm diameter lipid vesicles. Scale bars are 20 μm.

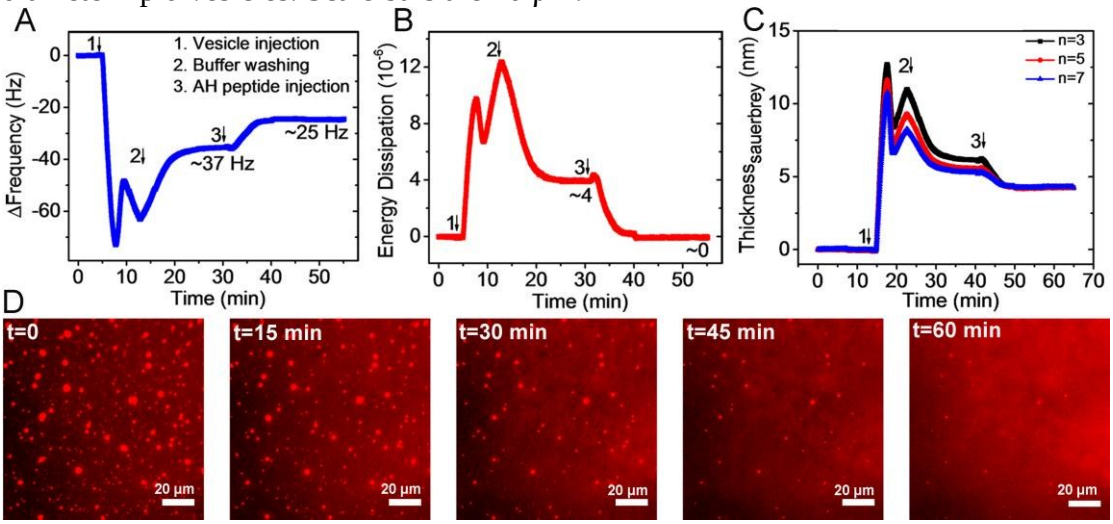

Figure 3. FRAP micrographs of SLB showing pre- and post-repair by AH peptide. Each post bleaching micrograph is shown at 30 sec interval. Scale bar represents 10 μm.

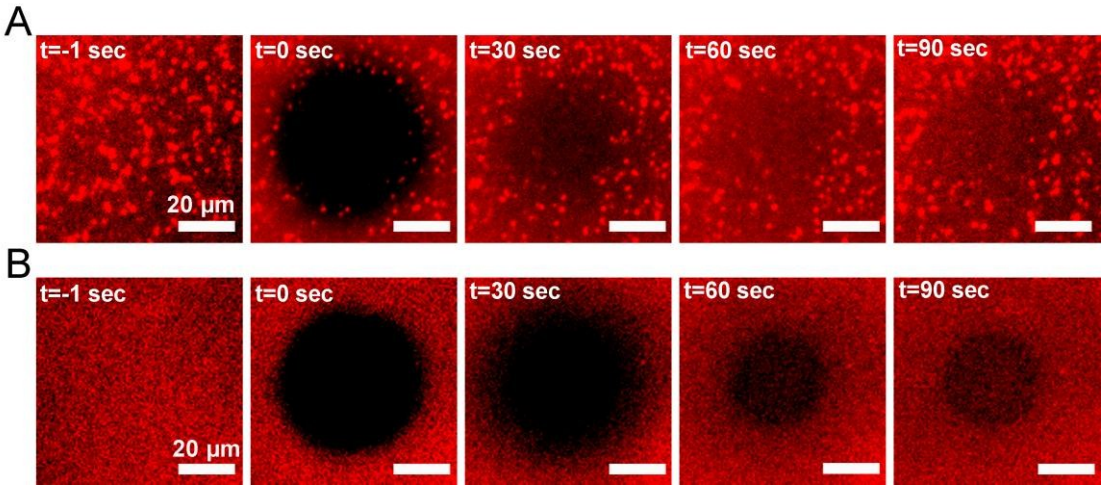

Figure 4. Influence of vesicle size on AH peptide-mediated SLB repair. Kinetic profiles of repairing on various sizes of vesicles were monitored by QCM-D. After the rupture of each different size of vesicles, **(A)** changes in resonant frequency and **(B)** energy dissipation at third overtone were normalized at t = 0 min. Arrows indicate injection of AH peptide.

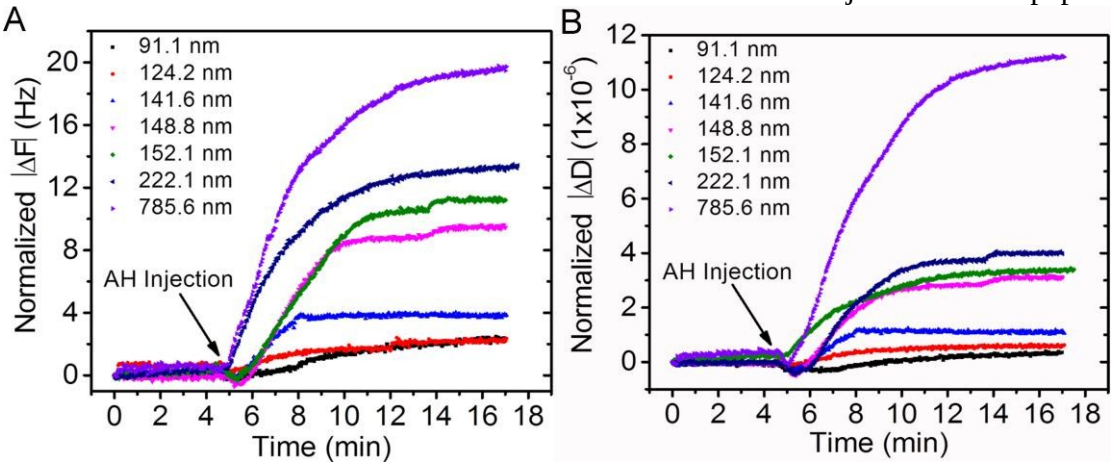

Figure 5. Time-lapse fluorescence micrographs of AH peptide-mediated SLB repair. (A-C) Fluorescence micrographs of bilayer repair process as a function of vesicle size. Scale bars are 20 µm. **(D)** Number of unruptured vesicles before and after AH peptide treatment.

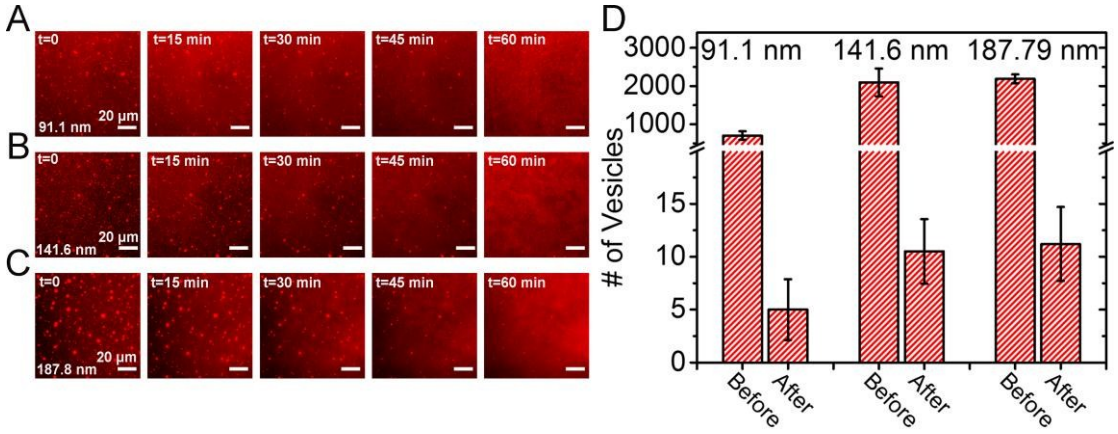

Table 1. Summary table for supported lipid bilayer repair mediated by AH peptide. Initial/final changes in resonance frequency and energy dissipation at third overtone before and after the repair are reported as a function of extrusion filter size. To note that each subscript value 1 indicates before the repair while the value 2 corresponds to the final kinetic values after the repair. The numbers with asterisk indicate how many times vesicle containing solutions were passed through the extrusion membrane filters.

Extrusion Filter Size (nm)	DLS Measurement Size (nm)	Polydispersity	ΔF_1 (Hz)	ΔF_2 (Hz)	ΔD_1 (1×10^{-6})	ΔD_2 (1×10^{-6})
50 (23*)	91.0 ± 0.2	0.079	28.78	26.37	0.5122	0.1576
100 (23*)	128.7 ± 0.7	0.058	28.82	26.34	0.5836	0.0137
100 (17*)	141.3 ± 0.7	0.078	29.75	26.13	1.0941	0.0126
100 (13*)	148.5 ± 0.6	0.092	37.01	27.63	3.2182	0.1286
100 (7*)	151.8 ± 1.2	0.093	38.39	27.00	3.5131	0.2933
200 (13*)	221.3 ± 1.4	0.173	37.16	25.00	4.0272	0.0127
400 (7*)	784.9 ± 12.9	0.347	46.34	26.25	11.4280	0.0469

References

1. E. Sackmann, *Science*, 1996, 271, 43-48.
2. Y. H. Chan and S. G. Boxer, *Current Opinion in Chemical Biology*, 2007, 11, 581-587.
3. H. Jung, A. D. Robison and P. S. Cremer, *Journal of the American Chemical Society*, 2009, 131, 1006-1014.
4. J. H. Jeong, J.-H. Choi, M. C. Kim, J. H. Park, J. S. Herrin, S. H. Kim, H. Lee and N.-J. Cho, *European Biophysics Journal*, 2015, 1-9.
5. M. L. Wagner and L. K. Tamm, *Biophysical Journal*, 2001, 81, 266-275.
6. S. Yorulmaz, S. R. Tabaei, M. Kim, J. Seo, W. Hunziker, J. Szebeni and N.-J. Cho, *European Journal of Nanomedicine*, 2015, 7, 245-255.
7. J. C. Munro and C. W. Frank, *Langmuir*, 2004, 20, 10567-10575.
8. O. Purrucker, A. Förtig, R. Jordan and M. Tanaka, *ChemPhysChem*, 2004, 5, 327-335.
9. J. A. Jackman, W. Knoll and N.-J. Cho, *Materials*, 2012, 5, 2637-2657.
10. W. Römer and C. Steinem, *Biophysical Journal*, 2004, 86, 955-965.
11. D. Weiskopf, E. K. Schmitt, M. H. Klühr, S. K. Dertinger and C. Steinem, *Langmuir*, 2007, 23, 9134-9139.
12. P. S. Cremer and S. G. Boxer, *Journal of Physical Chemistry B*, 1999, 103, 2554-2559.
13. I. Reviakine and A. Brisson, *Langmuir*, 2000, 16, 1806-1815.
14. T. H. Anderson, Y. Min, K. L. Weirich, H. Zeng, D. Fygenson and J. N. Israelachvili, *Langmuir*, 2009, 25, 6997-7005.
15. N. J. Cho, C. W. Frank, B. Kasemo and F. Höök, *Nature Protocols*, 2010, 5, 1096-1106.
16. N. Vila, M. Puggelli and G. Gabrielli, *Colloids and Surfaces A: Physicochemical and Engineering Aspects*, 1996, 119, 95-104.
17. S. R. Tabaei, J.-H. Choi, G. Haw Zan, V. P. Zhdanov and N.-J. Cho, *Langmuir*, 2014, 30, 10363-10373.
18. S. R. Tabaei, J. A. Jackman, S.-O. Kim, B. Liedberg, W. Knoll, A. N. Parikh and N.-J. Cho, *Langmuir*, 2014, 30, 13345-13352.

19. S. R. Tabaei, S. Vafaei and N.-J. Cho, *Physical Chemistry Chemical Physics*, 2015, DOI: 10.1039/C5CP01428J.

20. J. A. Jackman, S. R. Tabaei, Z. Zhao, S. Yorulmaz and N.-J. Cho, *ACS Applied Materials & Interfaces*, 2015, 7, 959-968.

21. S. R. Tabaei, J. A. Jackman, S.-O. Kim, V. P. Zhdanov and N.-J. Cho, *Langmuir*, 2015, 31, 3125-3134.

22. S. R. Tabaei, J. A. Jackman, B. Liedberg, A. N. Parikh and N.-J. Cho, *Journal of the American Chemical Society*, 2014, 136, 16962-16965.

23. L. K. Tamm and H. M. McConnell, *Biophys. J.*, 1985, 47, 105-113.

24. C. Keller and B. Kasemo, *Biophys. J.*, 1998, 75, 1397-1402.

25. J. A. Jackman, N.-J. Cho, R. S. Duran and C. W. Frank, *Langmuir*, 2009, 26, 4103-4112.

26. J. A. Jackman, J.-H. Choi, V. P. Zhdanov and N.-J. Cho, *Langmuir*, 2013, 29, 11375-11384.

27. S. Boudard, B. Seantier, C. Breffa, G. Decher and O. Felix, *Thin Solid Films*, 2006, 495, 246-251.

28. E. Reimhult, F. Höök and B. Kasemo, *Physical Review E: Statistical, Nonlinear, and Soft Matter Physics*, 2002, 66, 051905.

29. N.-J. Cho, J. A. Jackman, M. Liu and C. W. Frank, *Langmuir*, 2011, 27, 3739-3748.

30. B. Seantier and B. Kasemo, *Langmuir*, 2009, 25, 5767-5772.

31. S. Terrettaz, M. Mayer and H. Vogel, *Langmuir*, 2003, 19, 5567-5569.

32. N.-J. Cho, S.-J. Cho, K. H. Cheong, J. S. Glenn and C. W. Frank, *Journal of the American Chemical Society*, 2007, 129, 10050-10051.

33. N.-J. Cho, G. Wang, M. Edvardsson, J. S. Glenn, F. Hook and C. W. Frank, *Analytical chemistry*, 2009, 81, 4752-4761.

34. G. H. Zan, J. A. Jackman and N.-J. Cho, *Journal of Physical Chemistry B*, 2014, 118, 3616-3621.

35. N.-J. Cho, S.-J. Cho, J. O. Hardesty, J. S. Glenn and C. W. Frank, *Langmuir*, 2007, 23, 10855-10863.

36. N.-J. Cho, K. K. Kanazawa, J. S. Glenn and C. W. Frank, *Analytical Chemistry*, 2007, 79, 7027-7035.

37. J. A. Jackman, G. H. Zan, V. P. Zhdanov and N.-J. Cho, *Journal of Physical Chemistry B*, 2013, 117, 16117-16128.

38. G. H. Zan and N.-J. Cho, *Colloids and Surfaces B: Biointerfaces*, 2014, 121, 340-346.

39. G. J. Hardy, R. Nayak, S. M. Alam, J. G. Shapter, F. Heinrich and S. Zauscher, *Journal of Materials Chemistry*, 2012, 22, 19506-19513.

40. J. Wang, K.-W. Liu and S. L. Biswal, *Analytical Chemistry*, 2014, 86, 10084-10090.

41. S. R. Tabaei, M. Rabe, V. P. Zhdanov, N.-J. Cho and F. Höök, *Nano Letters*, 2012, 12, 5719-5725.

42. N.-J. Cho, H. Dvory-Sobol, A. Xiong, S.-J. Cho, C. W. Frank and J. S. Glenn, *ACS Chemical Biology*, 2009, 4, 1061-1067.

43. J. A. Jackman, R. Saravanan, Y. Zhang, S. R. Tabaei and N. J. Cho, *Small*, 2015, 11, 2372-2379.

44. R. C. MacDonald, R. I. MacDonald, B. P. M. Menco, K. Takeshita, N. K. Subbarao and L.-r. Hu, *Biochimica et Biophysica Acta (BBA)-Biomembranes*, 1991, 1061, 297-303.

45. P. Jönsson, M. P. Jonsson, J. O. Tegenfeldt and F. Höök, *Biophysical Journal*, 2008, 95, 5334-5348.

46. R. P. Richter, R. Bérat and A. R. Brisson, *Langmuir*, 2006, 22, 3497-3505.

47. E. Reimhult, F. Höök and B. Kasemo, *Langmuir*, 2003, 19, 1681-1691.

48. P. Bingen, G. Wang, N. F. Steinmetz, M. Rodahl and R. P. Richter, *Analytical Chemistry*, 2008, 80, 8880-8890.

49. K. Glasmästar, C. Larsson, F. Höök and B. Kasemo, *Journal of Colloid and Interface Science*, 2002, 246, 40-47.

Table of Contents Entry

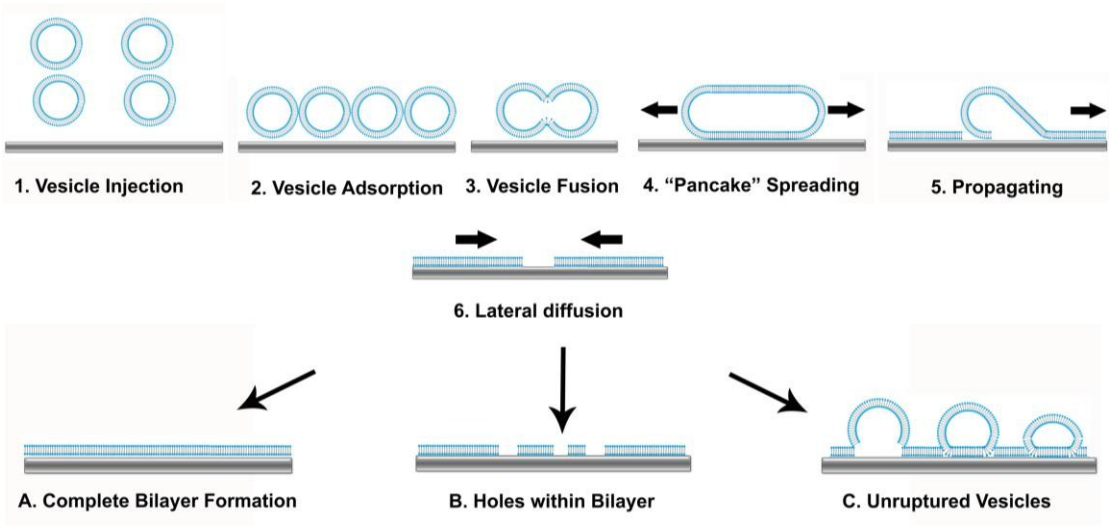

High-quality and complete supported lipid bilayers are formed on silicon oxide by employing an AH peptide-mediated repair step.